Effect of hydroxyl groups on erbium-doped bismuth-oxide-based glasses for fiber amplifiers

Hideaki Hayashi[a)]
Research Center, Asahi Glass Co., Ltd., Yokohama 221-8755, Japan and Graduate School of Human and Environmental Studies, Kyoto University, Kyoto 606-8501, Japan

Naoki Sugimoto
Research Center, Asahi Glass Co., Ltd., Yokohama 221-8755, Japan

Setsuhisa Tanabe
Graduate School of Human and Environmental Studies, Kyoto University, Kyoto 606-8501, Japan

Seiki Ohara
Research Center, Asahi Glass Co., Ltd., Yokohama 221-8755, Japan

(Received 14 January 2006; accepted 7 March 2006; published online 12 May 2006)

The interactions between Er^{3+} ions OH groups in Er-doped Bi_2O_3-based glasses were investigated for samples with various Er OH concentrations. From the analyses of the total decay rate of the $^4I_{13/2}$ level of Er^{3+} it was confirmed that the OH groups are dominant quenching centers of excited Er^{3+} and a cause of concentration quenching of 1.5 μm band emission. The attempts to remove the OH groups in the melting process were then performed. Highly dehydrated glass was obtained by keeping the dew point of the melting atmosphere at the order of −30 °C. The solution of the OH groups in reheating processes for fiber fabrication was also investigated. It was revealed that they diffused from the glass surface to the inside with an order of millimeters when the glasses were annealed above softening temperature. Finally, we fabricated highly Er-doped, 5 cm length compact *C*-band fiber amplifiers with various OH concentrations. By removing the OH groups in the core glasses, the gain characteristics drastically improved and a 10 dB gain at 1560 nm was achieved with 150 mW pumping at 980 nm. © *2006 American Institute of Physics*.
[DOI: 10.1063/1.2192267]

I. INTRODUCTION

In order to meet demand for the exponential increase of information capacity, considerable research efforts have been made to develop optical amplifiers for wavelength division multiplexing (WDM) network system.[1] As practical amplification medium, Er^{3+}-doped fibers have been extensively studied due to their excellent gain operation around 1.5 μm in a loss minimum window of transmission silica fiber. Recently, as a result of the development of optical network system such as optical cross connect and optical add drop in metro and access, integration and cost reduction of each device at the network nodes have been needed. To meet these demands, compact amplifiers such as short-length fiber amplifiers or Er-doped planar waveguide amplifiers have been proposed.[2–5] For the amplifiers with the short effective length, it is necessary that the doping concentration of Er^{3+} ions in the devices is sufficiently high. As glass hosts for the amplification of Er^{3+}, silica-based glasses have been used, however, it is reported that the concentration quenching of Er^{3+} ions begins at less than 1000 wt ppm.[6,7] Therefore the effective length of the silica-based amplifier becomes relatively long. As candidates of the materials for optical amplifiers, we have developed Er^{3+}-doped Bi_2O_3-based glasses.[8] They have quite large emission and absorption cross sections because of their high refractive indices of the hosts of more than 2.0.[8,9] In addition, for the Bi_2O_3-based glass systems, the stable glasses can be obtained with higher Er_2O_3 concentrations. Thus it is expected that the gain coefficients (dB/cm) of the amplifiers using these materials will be much higher than the silica-based ones. Moreover, the materials show flat and broad $^4I_{13/2}$-$^4I_{15/2}$ emission of Er^{3+} ion around 1.5–1.6 μm, so they have a potential for excellent amplifiers in the WDM network.

It is known that free-OH groups, whose fundamental vibration ranges between 2500 and 3600 cm^{-1}, are one of the dominant quenching centers in Er^{3+}-doped glasses.[10,11] Since the energy gap between the $^4I_{13/2}$ and $^4I_{15/2}$ levels (6500 cm^{-1}) approximately corresponds to the energy of overtone of the free-OH stretching vibration, nonradiative relaxation from $^4I_{13/2}$ can occur when an Er^{3+} ion is coupled to a OH group. Many studies have been carried out on the quenching effect of the OH groups in optically Er-doped glass systems such as silicate, phosphate, and tellurite.[10–16] However, it is not clear how the OH groups act in the Er-doped Bi_2O_3-based glasses in spite of their excellent 1.5 μm band emission properties. In this study, the effect of the OH groups on the total decay rate of the Er^{3+}:$^4I_{13/2}$ level in the Bi_2O_3-based glasses is investigated to reveal the interaction between the Er^{3+} ions and the OH groups. The attempts to remove the OH groups in the melting processes were then performed with several conditions. In addition, solution and diffusion of the OH groups in fiber fabricating processes

[a)]Electronic mail: hideaki-hayasi@agc.co.jp

such as forming of glass preform and drawing were investigated because the solution of water to the glasses may be a problem when its concentration in the atmosphere is higher than that in the glass inside. The solution of the OH groups in the processes was tested by the reheating of the dehydrated glasses. The diffusion of the OH groups at core-cladding interface was also investigated to reveal whether the dehydration of the Bi_2O_3-based glass for the fiber cladding is also needed or not. Another purpose of this study is to clarify how the OH groups affect the gain characteristics of Er-doped fiber (EDF) as actual amplification media. Highly Er-doped Bi_2O_3-based glass fibers (BIEDFs) with 5 cm length are fabricated for compact C-band amplifiers with various OH concentrations, and the variations of the gain characteristics are experimentally and theoretically studied.

II. EXPERIMENT

A. Sample preparation

The Bi_2O_3-based glasses were prepared using conventional melting methods. Two representative compositions were selected here. One composition contains Bi_2O_3 and SiO_2 as constituents (type *A*), and another contains B_2O_3 in addition to the above oxides (type *B*). For the fiber core composition, Er_2O_3 was added to the glass batch (0.5, 1, or 2 mol %). The following five melting conditions were performed to remove the OH groups in the glasses. All the samples were melted in the ambient pressure. In procedure I, the samples were melted in the air atmosphere and in procedure II, they were done with flows of dry N_2 gases. The N_2 gases were also flown from procedures III to V; however, they were different from procedure II in the following points. For procedure III, CCl_4 gases were further introduced into the atmosphere by the bubbling of the liquid material at 40 °C.[10,11] For procedure IV, $BiCl_3$ chemicals were directly added to the glass batches with the substitution of $1/2$ Bi_2O_3. In the case of procedure V, the samples were melted in a sealed chamber. By flowing dry air gas, the dew point temperature of this chamber was kept at −35 °C. In the experiments comparing the effects of melting conditions, all the glasses were melted on the same day. After 1 h melting, the 300 g of glass melts in a crucible were cast into a carbon mold. The glass samples were then annealed at 10 °C above the glass transition temperature for 1 h (400–540 °C). The annealed glass samples were cut into $18\times15\times3.5$ mm^3 in size and polished for optical measurements.

In order to evaluate the glass materials as optical amplification media, single mode EDFs (cladding diameter of 125 μm) with plastic coatings were fabricated using the glasses described above. Er_2O_3 doping concentration in the core was 1 mol % (13 000 wt ppm as Er), and the fiber length was set to 5 cm. The mode field diameter at 1550 nm was 4 μm. The refractive index of the core and the numerical aperture (NA) of the fiber at 1550 nm were 2.03 and 0.20, respectively. By using a cutback method, the propagation loss at 1310 nm was estimated to be 0.6 dB/m. The BIEDFs were fusion spliced to high NA fibers (Corning HI980) using a commercial fusion splicer and the average splice loss was estimated to be 0.5 dB/point. Angled cleaving and splicing were applied to suppress the reflection due to the large difference of refractive inducis between the BIEDFs and the silica fibers. All the bare pig-tailed BIEDFs passed Bellcore (Telcordia) GR-1221 CORE qualification test.[17]

B. Optical measurements

Absorption spectra of the Er-doped glasses were measured using an UV-visible near-infrared (UV-VIS-NIR) recording spectrophotometer (U-3500, Hitachi, Ltd.) in the range of 300–3200 nm. The absorption of the OH groups was evaluated using α_{OH}, which is represented by the peak of absorption coefficient around 3.0 μm band that was attributed to OH vibration.[14] For luminescence decay measurements, a 980 nm diode laser (HPD-112-T03-TEC, High Power Device Inc.) was modulated into pulses using a function generator ($f=20$ Hz, $\Delta\tau=50$ μs). An In–Ga–As photodiode ($f=160$ kHz; model IGA-020-A, Electro-Optical Systems) was used as a detector for the decay measurements of the Er^{3+}:$^4I_{13/2}$ level. The luminescence was monochromated, and the decay curve for the overlapped signal was deconvoluted. The signal of the photodiode was collected using a digital oscilloscope (500 MHz; model TDS520, Tectronix), and the lifetime was determined by least-squares fitting of the decay curve with exponential functions. In this paper, the total decay rate W_{total} ($=1/\tau_f$, τ_f the lifetime of the $^4I_{13/2}$ level) was mainly used for the analyses of relaxation behavior of excited Er^{3+} ions.

C. Reheating test

The dehydrated glass samples ($\alpha_{OH}=0.41$) of $18\times15\times8$ mm^3 in size were set onto stainless mold with the smallest face of the cubic sample to be contacted with the mold, and then annealed at 550 °C in the air atmosphere. The dehydration method at the melting process was the same as procedure V. To investigate the distribution of the OH groups in the glasses, each reheated sample was polished by degrees from the top surface of the largest face, and the variation of the α_{OH} in the residual sample was examined every time after one polishing. We also investigated the diffusion of the OH groups at core-cladding interface as follows. The core glass melt that was prepared in the dry atmosphere ($\alpha_{OH}=0.52$) was poured onto the cladding bulk glass of $18\times15\times8$ mm^3 in size which was prepared in the air atmosphere ($\alpha_{OH}=3.0$). The obtained glass composite was then annealed at 550 °C for 6 h in the air atmosphere. The annealed sample was polished by degrees from the core side and absorption measurements were performed.

D. Gain simulations and measurements of BIEDF

In order to estimate the effect of the OH groups in the core glasses on the gain characteristics of the BIEDF theoretically, we describe rate equations to analyze the population dynamics of Er^{3+} ions, and the lightwave propagation equation along the BIEDF.[18,19] Figure 1 shows the energy level diagram of Er^{3+} ion and relevant transitions when pumped at 980 nm. For simplicity, we neglect the intermediate levels between the $^4I_{11/2}$ and $^4F_{7/2}$ levels, and assume that

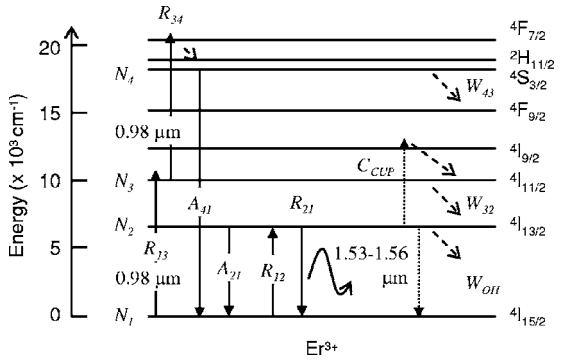

FIG. 1. Energy level diagram of Er^{3+} ion and relevant transitions when pumped at 980 nm.

all the photons pumped at the $^4F_{7/2}$ level via excited-state absorption transit nonradiatively to $^4S_{3/2}$ then emit spontaneously to the ground $^4I_{15/2}$ level. In this case, the rate equations for the Er^{3+} ion population at each level can be expressed as follows:

$$dN_1/dt = (A_{21} + R_{21})N_2 - (R_{13} + R_{12})N_1 + W_{OH}N_{OH}N_2 + C_{CUP}N_2^2 + A_{41}N_4, \quad (1)$$

$$dN_2/dt = -(A_{21} + R_{21})N_2 + R_{12}N_1 + W_{32}N_3 - W_{OH}N_2 - 2C_{CUP}N_2^2, \quad (2)$$

$$dN_3/dt = R_{13}N_1 - (W_{32} + R_{34})N_3 + W_{43}N_4 + C_{CUP}N_2^2, \quad (3)$$

$$dN_4/dt = -(A_{41} + W_{43})N_4 + R_{34}N_3, \quad (4)$$

where N_1, N_2, N_3, and N_4 represent the population of the $^4I_{15/2}$, $^4I_{13/2}$, $^4I_{11/2}$, and $^4F_{7/2}$ levels, respectively. Total Er concentration for the calculation was set to 13 000 wt ppm. R_{21}, R_{12}, R_{13}, and R_{34} are radiation transition rates between these levels that were calculated from absorption and emission cross sections (σ_e^s, σ_a^s, σ_a^p, and σ_{ESA}, respectively). A_{21} and A_{41} represent spontaneous emission probabilities that were calculated by the Fuchtbauer-Ladenburg formula.[20] W_{32} and W_{43} represent nonradiative decay rates that were estimated from the lifetime measurements of the bulk glasses. W_{OH} is the relaxation rate via the OH groups (it is explained in the following section). The fiber length, the mode field diameter, and the NA were set to 5 cm, 4 μm, and 0.20, respectively. From the empirical energy gap law, we assume W_{21} and A_{31} to be zero. Homogeneous two-particle upconversion model is applied, so the cooperative upconversion term is expressed as $C_{CUP}N_2^2$, where C_{CUP} is upconversion coefficient.[21] For the estimation of the C_{CUP}, the relative intensity of the $^4S_{3/2} \rightarrow {}^4I_{15/2}$ transition (0.55 μm band) to the $^4I_{13/2} \rightarrow {}^4I_{15/2}$ transition (1.53 μm band) in the BIEDF pumped at 980 nm was experimentally investigated. When we denote each emission intensity as $P_{0.55}$ and $P_{1.53}$, they are related as $P_{0.55} \propto A_{41}N_4$ and $P_{1.53} \propto A_{21}N_2$, respectively, and the relative intensity of these transitions can be calculated by assuming the steady state condition in Eqs. (1)–(4). The C_{CUP} was then estimated by fitting the calculated relative intensity to the experimental one.

TABLE I. Parameters used for numerical calculations (type *A* glass-based fiber).

Parameter	Symbol	Value	Unit
Spontaneous emission rate	A_{21}	385	s^{-1}
	A_{41}	2 800	s^{-1}
Nonradiative decay rate	W_{32}	7 500	s^{-1}
	W_{43}	75 000	s^{-1}
Relaxation rate via OH group	W_{OH}	6.2×10^{-24}	m^3/s
Cooperative upconversion coefficient	C_{CUP}	8.5×10^{-24}	m^3/s
Signal emission cross section at 1560 nm	σ_s^e	4.82×10^{-25}	m^2
Signal absorption cross section at 1560 nm	σ_s^a	2.42×10^{-25}	m^2
Pump absorption cross section at 980 nm	σ_p^a	2.36×10^{-25}	m^2
Er^{3+} ion density	N	3.16×10^{26}	m^{-3}

The signal and pump lightwaves propagating along the fiber (I_s and I_p, respectively) are expressed as the following set of ordinary differential equations.[18]

$$dI_s/dz = (\sigma_s^e N_2 - \sigma_s^a N_1)I_s, \quad (5)$$

$$dI_p^{\pm}/dz = \mp(\sigma_p^a N_1 \mp \sigma_p^e N_3 \pm \sigma_{ESA}N_3)I_p. \quad (6)$$

Here we applied Quimby's assumption that σ_{ESA} is equal to $2\sigma_p^a$.[22] We made approximations with regard to modal overlaps to simplify the approach (confinement factor was equal to unity). In addition, a uniform distribution of Er^{3+} ion in the core was assumed. Although spontaneous decay was accounted for, amplified spontaneous emission (ASE) was neglected since the input signal power was sufficiently large (0 dB m) and the fiber length was extremely short. We also neglected the insertion loss since the background loss of this 5 cm fiber was typically 0.5 dB/m and a splice loss from BIEDF to high NA silica fiber was less than 0.5 dB/point with conventional automatic splicer. Assuming a steady state condition (the time derivatives to be zero), the set of differential equations are numerically integrated using the fourth-order Runge-Kutta method with an initial condition at the input end and output end of the fiber ($z=0$ and $z=0.05$ m, respectively). The boundary value problem was solved by shooting method. The parameters used for numerical calculations are shown in Table I.

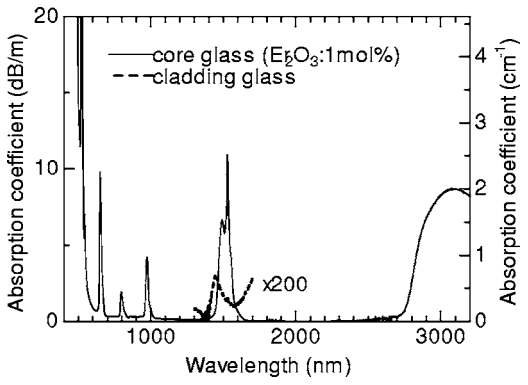

FIG. 2. Absorption spectra of the Bi_2O_3-based glass (type *A*) doped with 1 mol % of Er_2O_3 (solid line) and the glass for a cladding (dashed line). The left axis indicates absorption coefficient in the unit of dB/m, and the right axis in cm^{-1}.

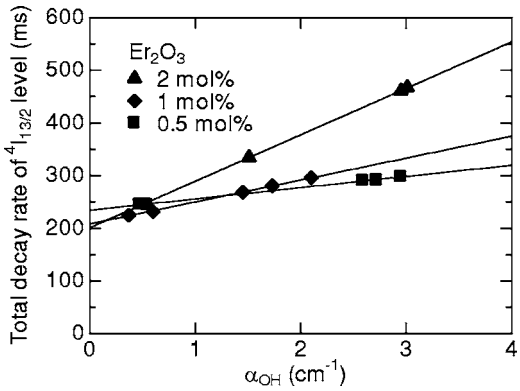

FIG. 3. Variation of the total decay rate of the $^4I_{13/2}$ level as a function of the α_{OH} in the Bi_2O_3-based glasses (type *A*) doped with 0.5, 1, and 2 mol % of Er_2O_3.

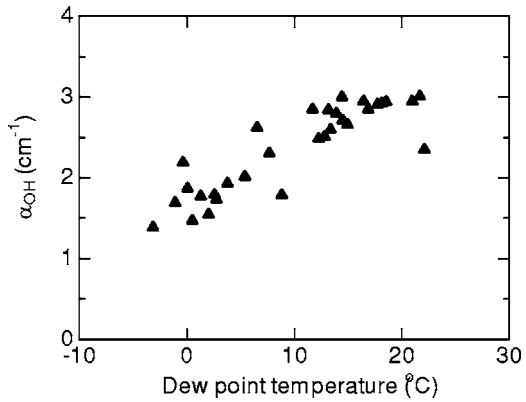

FIG. 5. Relationship between the α_{OH} in the Bi_2O_3-based glasses and the dew point temperature of the atmosphere.

Using the parameters as described above, we examine the effect of the OH groups on the gain characteristics of BIEDFs. The experimental results are compared with the theoretical ones. For the gain measurements, 5 cm length fibers were bidirectionally pumped with 280 mW (140 mW per laser diode) at the wavelength of 980 nm. A tunable laser (model TL-210, Santec Corp.) in the wavelength range of 1520–1620 nm was input from the forward end of the BIEDF as a signal source. Input signal powers were set to 0 dB m. The amplified signals at the output end were collected using an optical spectrum analyzer (model AQ6317B, Ando Electric Co., Ltd.) with a 0.05 nm resolution.

III. RESULTS

A. Effect of OH groups on bulk properties

Absorption spectra of the Bi_2O_3-based glass doped with 1 mol % of Er_2O_3 (type *A*, for a fiber core) and the glass without Er_2O_3 (for a fiber cladding) are shown in Fig. 2. These glasses were melted with procedure I. For the core glass, the attenuation at the absorption peak of the 1.5 μm band was 1100 dB/m. The absorption peak of 3.0 μm band was comparable with that of the 1.5 μm band. For the glass without Er_2O_3, the small absorption peak around 1.4 μm was observed. Figure 3 shows the variation of the total decay rate of the $^4I_{13/2}$ level as a function of the α_{OH} in the Bi_2O_3-based glasses (type *A*) doped with 0.5, 1, and 2 mol % of Er_2O_3. For each Er_2O_3 concentration, the total decay rate W_{total} increased linearly with the α_{OH}. In addition, we can see that the slope of the fitting lines increased with the Er_2O_3 concentrations. The values of the *y* intercept for the glasses with 0.5, 1, and 2 mol % of Er_2O_3 were 235, 209, and 201 s^{-1}, respectively.

Variation of the OH groups with melting conditions and processes is shown in Figs. 4–6. Figure 4 shows absorption spectra of the Bi_2O_3-based glasses (type *A*) with several melting conditions as described in the Experiment section. When melted in the air atmosphere, the α_{OH} of the obtained glass was 3.45 (procedure I). By flowing dry N_2 gas, the α_{OH} decreased to 2.90 (procedure II). In the case of introducing CCl_4 and BCl_3, the α_{OH} decreased to 2.44 and 1.61, respectively (procedures III and IV). When melted in a sealed chamber, the α_{OH} decreased to 0.44 (procedure V). Figure 5 shows the relationship between the α_{OH} of the Bi_2O_3-based glasses (type *A*) and the dew point temperature of the atmosphere. Here all the glasses were melted in the air atmosphere on different days, and each plot in the graph corresponds to a melting date. The α_{OH}'s of the glasses are different with the melting dates. We can see that there is a positive correlation between the α_{OH} and the dew point temperature. Figure 6 shows the variation of the α_{OH}'s of the

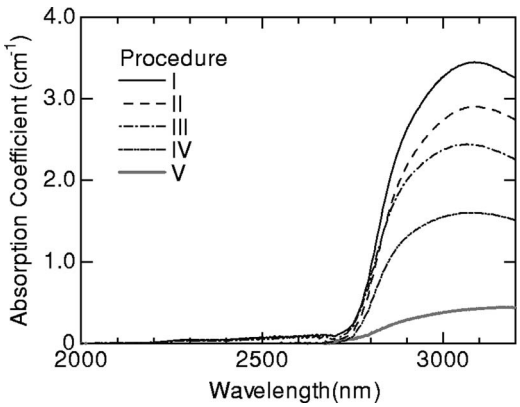

FIG. 4. Absorption spectra of Bi_2O_3-based glasses with several melting conditions. Procedure I: in the air atmosphere. Procedure II: in the air atmosphere with N_2 flow. Procedure III: in the air atmosphere with N_2 flow and CCl_4 bubbling. Procedure IV: in the air atmosphere with N_2 flow and BCl_3 additive. Procedure V: in a sealed chamber with dry air flow.

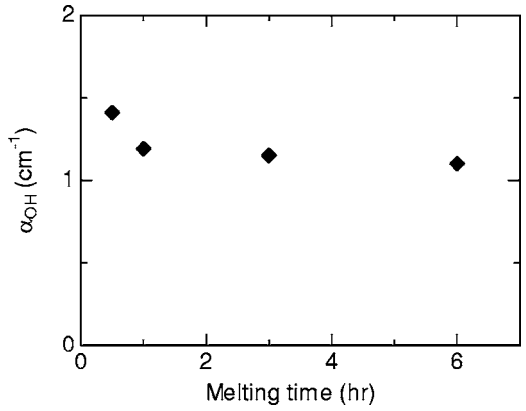

FIG. 6. Variation of the α_{OH} in the Bi_2O_3-based glasses with melting time.

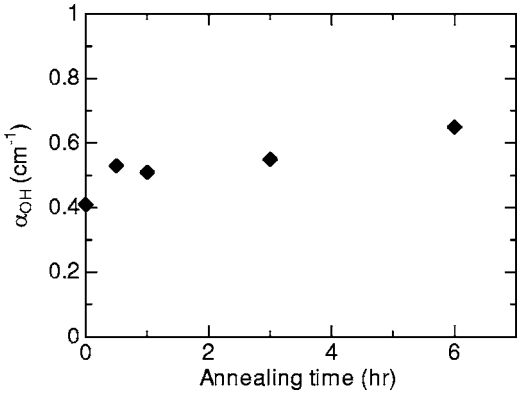

FIG. 7. Variation of the α_{OH} in the Bi_2O_3-based glasses with reheating time. The dehydrated samples (α_{OH}=0.41) were annealed in the air atmosphere at 550 °C.

type *A* glasses with melting time. In this case, each glass batch was 30 g, and they were melted in identical condition (procedure I). We can see that the α_{OH} decreased with the melting time and almost saturated to the constant value when melted for 6 h.

Variation of the α_{OH} in reheating process is shown in Figs. 7 and 8. Figure 7 shows the variation of the α_{OH}'s of the dehydrated Bi_2O_3-based glasses (type *A*, α_{OH}=0.41) with reheating time. As shown in the figure, the α_{OH} increased with the reheating time when annealed at 550 °C. The distribution of the OH groups in these samples is investigated as described in the Experiment section. Figure 8 shows the relationship between polishing amount from the top surface of the annealed samples (annealed for 0.5, 1, 3, or 6 h) and the α_{OH} of residual part. As the polishing advanced, the α_{OH}'s of the residual glasses increased. In addition, as the annealing time became longer, the increase was larger. Furthermore, the polishing amount that the α_{OH} started to increase was smaller for samples annealed for longer times.

B. Effect of OH groups on gain characteristics of BIEDF

The gain characteristics of 5 cm length fibers were experimentally measured. In addition, using the parameters obtained in Sec. II D, we can investigate the effect of the OH groups on the gain characteristics of the BIEDF theoretically.

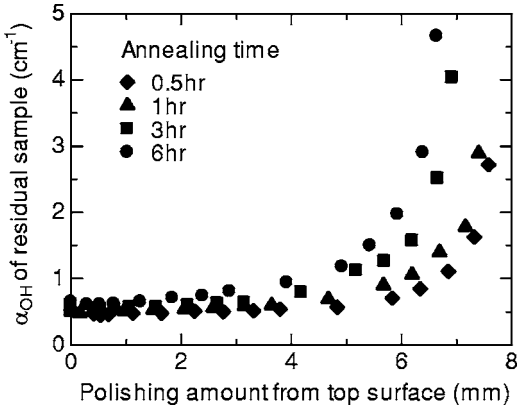

FIG. 8. Relationship between polishing amount from the top surface of the annealed glass samples (0.5, 1, 3, or 6 h) and the α_{OH} of residual part.

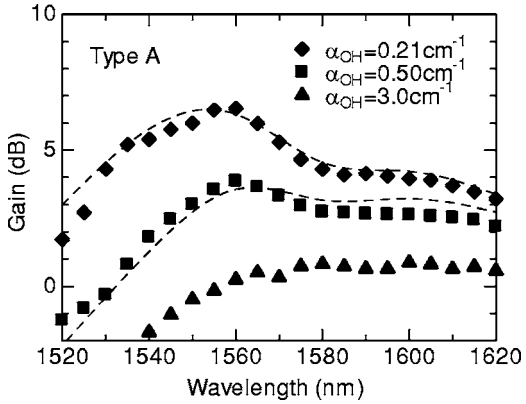

FIG. 9. Gain profiles of BIEDFs (type *A* glass based) for different OH concentrations. Dashed lines represent simulation results. 5 cm length fibers are bidirectionally pumped with 280 mW at 980 nm. Input signal power is 0 dBm.

Figure 9 shows the experimental and simulation gain profiles with different OH concentrations (type *A* glass-based fiber). For the case of 1 mol % of Er_2O_3 (13 000 wt ppm as Er), we can see that gain was hardly reached without atmosphere control (α_{OH}=3.0). When the α_{OH} of the core glass decreased to 0.21, the internal gain improved by more than 6 dB at 1560 nm in the 5 cm fiber. Turning now to the simulation results, it can be seen that the numerical gain profiles fit the experimental ones. As for the BIEDF using the type *B* core glass (B_2O_3 contained), the same behaviors were also observed for both the experiments and simulations. Figure 10 shows the gain curve of the types *A* and *B* glass-based fibers at 1560 nm. The better results were obtained in the type *B* glass-based fiber. For the type *B* glass-based fiber, the internal gain was reached at 10 dB with 150 mW pumping at 980 nm. The power conversion efficiency (PCE) of the fiber was 7%.

IV. DISCUSSION

A. Effect of α_{OH} on 1.5 μm band emission

The absorption peak around 1.5 μm in Fig. 2 corresponds to the Er^{3+}:$^4I_{15/2}$-$^4I_{13/2}$ transition. Since this peak is much greater than that in commercial Er-doped SiO_2-based fiber (generally at most around 30 dB/m), it can be said that

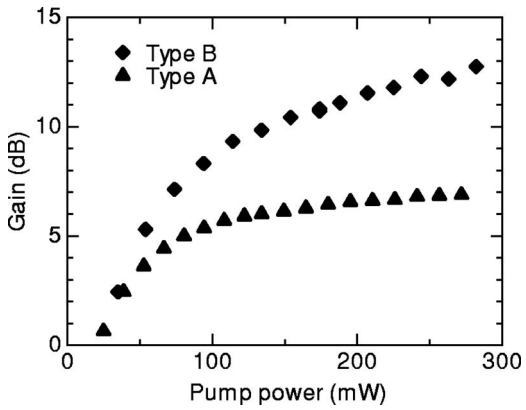

FIG. 10. Pump power dependence of gain at 1560 nm for BIEDFs pumped at 980 nm. Input signal power is 0 dBm.

the Bi_2O_3-based glass has a potential for short-length EDF with higher Er concentration and cross section of $4f$ transitions. The absorption peak around 3.0 μm must be identified as O–H stretching vibration. It is considered that at least a part of the OH groups is combined with Bi because the frequency of the peak in the Bi_2O_3-based glass is smaller than that in silica glass.[23] The 1.4 μm absorption band observed in the cladding glass should be attributed to the overtone of the free-OH stretching vibration. Since a part of this absorption band overlaps with the 1.5 μm emission band of Er^{3+}, nonradiative relaxation from $^4I_{13/2}$ will occur when an excited Er^{3+} ion is coupled to a OH group.

Next, we discuss the interaction between the Er^{3+} ions and OH groups in the Er-doped Bi_2O_3-based glasses. The total decay rate of the $^4I_{13/2}$ level of the Er^{3+} ions is represented by

$$W_{\text{total}} = \tau_f^{-1} = A + W_{\text{NR}}, \tag{7}$$

where W_{NR} is nonradiative decay rate that is decomposed as follows:

$$W_{\text{NR}} = W_{\text{OH}} + W_p + W_{\text{ET}} + \cdots, \tag{8}$$

where W_p is multiphonon decay rate, and W_{ET} is energy transfer rate among the Er^{3+} ions. The quantum efficiency of the $^4I_{13/2}$ level, η, is given by

$$\eta = A\tau_f. \tag{9}$$

For each Er concentration in Fig. 3, the total decay rate W_{total} increased linearly with the α_{OH}. Since the W_{total} is the function of the W_{OH}, it can be said from Eqs. (7)–(9) that the η will decrease with the increase of the α_{OH}. This indicates that the OH groups in the glasses are dominant quenching centers of the excited Er^{3+} ions. In the following discussions, we regarded all the OH groups to act as the quenching centers. In these experiments, this assumption must be valid because the Er concentration is extremely high. In addition, increase of the slope of the fitting line with the Er concentrations means that the OH groups are a cause of the concentration quenching.

From the linear relationship between the total decay rate of the $^4I_{13/2}$ level of Er^{3+} ion and the amount of the OH groups, we can estimate the interaction between an excited Er^{3+} ion and a OH group, W_{OH}. Snoeks *et al.* suggested that the deactivation of Er^{3+} ions by the OH groups occurs in the following process.[12] First, an excited Er^{3+} ion exchanges its energy with the neighbor ion at the ground state by radiative transfer. After the energy migration, the excitation energy is finally lost when it transfers to an Er^{3+} ion that coupled with a OH group. Based on the assumption, the probability of this process is represented as follows:[12]

$$W_{\text{OH}} = 8\pi C_{\text{Er–Er}} N_{\text{OH}} N_{\text{Er}}, \tag{10}$$

where $C_{\text{Er–Er}}$ is an interaction constant. N_{OH} and N_{Er} are the concentrations of the OH groups and Er^{3+} ions in the glass, respectively. Here we assume that all the Er–Er interaction is included in the $C_{\text{Er–Er}}$, and the W_{ET} in Eq. (8) to be zero. The OH content N_{OH} can be obtained by the following equation:[24]

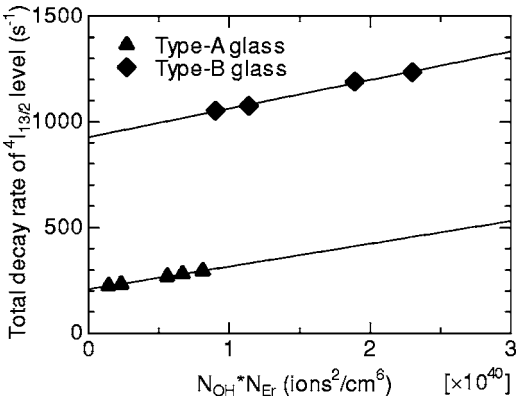

FIG. 11. Dependence of the total decay rate of the $^4I_{13/2}$ level on $N_{\text{OH}}N_{\text{Er}}$ in the types *A* and *B* glasses doped with 1 mol % of Er_2O_3.

$$N_{\text{OH}} = \frac{N_A}{\varepsilon L} \ln \frac{1}{T}, \tag{11}$$

where N_A is the Avogadro constant, L the glass thickness, T the transmittance, and ε the molar absorption coefficient of the OH groups in the glass. We applied the ε of silicate glasses (49.1×10^3 cm^2/mol),[25] since there is no relevant report about the Bi_2O_3-based glasses so far. Using Eqs. (7), (8), and (10), the total relaxation rate W_{total} is represented by

$$W_{\text{total}} = 8\pi C_{\text{Er–Er}} N_{\text{OH}} N_{\text{Er}} + k, \quad k = A_{\text{rad}} + W_p \cdots. \tag{12}$$

Figure 11 shows dependence of the W_{total} on $N_{\text{OH}}N_{\text{Er}}$ in the types *A* and *B* glasses. The plots are well fitted by straight-line functions. Since the k term in Eq. (12) is independent of the N_{OH}, we can calculate the $C_{\text{Er–Er}}$ from the slope of the fitting line. The $C_{\text{Er–Er}}$ of types *A* and *B* were 4.3×10^{-52} and 5.4×10^{-52} m^6/s, respectively. It is said that the moisture incorporated into a glass is coupled to glass-forming cations such as Si^{4+} or B^{3+}.[24] There should be a difference in OH sites between types *A* and *B*; however, it is not clear that the difference of the $C_{\text{Er–Er}}$ is the significant one. On the other hand, the difference of the W_{total} at $\alpha_{\text{OH}}=0$ is probably due to that of W_p. The W_p of the type *B* glass should be larger than that of type *A* because it contains B_2O_3 whose phonon energy is relatively large (1300 cm^{-1}).[26] The better results in the type *B* glass-based fiber are probably attributed to the larger phonon energy of the host glass. Since the lifetime of $^4I_{11/2}$ of Er^{3+} as the first pumped level should be smaller in the type *B* glass than that in type *A*, the effect of excited-state absorption on the type *B* glass is assumed to be smaller that on the type *A* glass. Table II shows the $C_{\text{Er–Er}}$ for various glasses that were taken from literatures.[12,13] The constant of the Bi_2O_3-based glass was smaller than that of the other

TABLE II. Er–Er interaction constants in various glasses.

Composition	$C_{\text{Er–Er}}$ (m^6/s)	Reference
Bi_2O_3-based glass (type *A*)	4.3×10^{-52}	
Bi_2O_3-based glass (type *B*)	5.4×10^{-52}	
Soda-lime glass	2.3×10^{-51}	12
Alkali borosilicate glass	8.6×10^{-52}	12
Phosphate glass	7.0×10^{-52}	13

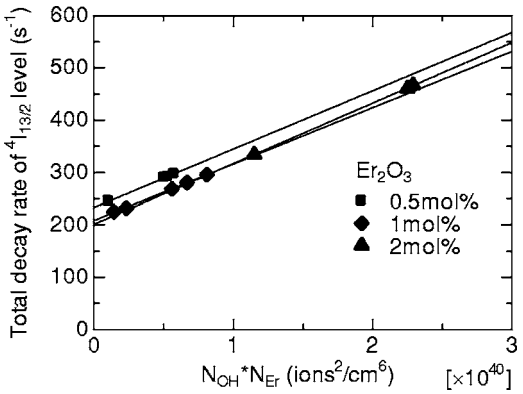

FIG. 12. Dependence of total decay rate of the $^4I_{13/2}$ level on $N_{OH}N_{Er}$ in the type *A* glasses doped with 0.5, 1, and 2 mol % of Er_2O_3.

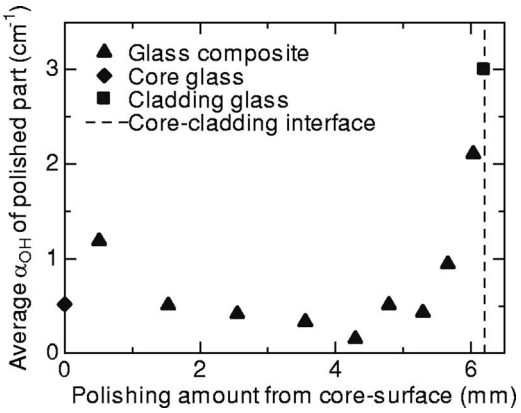

FIG. 13. Diffusion of the OH groups at the interface of composite of a water-rich cladding glass and a water-poor core glass.

glasses. This may be because the Er^{3+} ions are distributed more homogenously in the Bi_2O_3-based glasses than in the others. The good correspondence between experimental and simulation results of gain characteristics suggests that the C_{Er-Er} and W_{OH} parameters are appropriate. Figure 12 shows the W_{total} vs $N_{OH}N_{Er}$ of the type *A* glasses doped with 0.5, 1, and 2 mol % of Er_2O_3. In the same composition, the C_{Er-Er} was almost constant with the concentrations. From this result, we can say that the Er–Er interaction is independent of the concentration of both the Er^{3+} ions and the OH groups.

B. Solution of OH groups in melting process

First, from the difference between procedures I and II in Fig. 4, we can say that the flow of dry N_2 is effective for removing the OH group to some content. That of II and III or IV indicates the effect of chloride additives. Generally, dehydration by the chloride additives is expressed by the following chemical reaction:

$$XCl_a + bH_2O \rightarrow XO_b + aHCl\uparrow, \tag{13}$$

where *X* represents one chemical species, and *a* and *b* are coefficients. It is likely that the direct addition of chloride to the glass batch is more effective. From the result of sample V, we can say that the maintenance of highly dried atmosphere is one of the most important factors for the dehydration. The effect of the melting atmosphere is also suggested by the positive correlation between the water amount in the glasses and the dew point temperature of the atmosphere (Fig. 5).

C. Solution of OH group in reheating process

In Fig. 7, the increase of the α_{OH} indicates the solution of the OH groups from the air atmosphere to the glass inside in the reheating process. These α_{OH}'s represent the average water amount in the glasses since there should be the distribution of the OH groups until sufficient time for its complete diffusion. On the other hand, in Fig. 8, the increase of the α_{OH} should indicate the diffusion of water from the glass surface to the glass inside. It can be said that the distance of diffusion is in the order of millimeters for the annealed sample at 550 °C. Strictly speaking, we have to take the solution of water from the smaller faces of the cubic sample to the inside into account. However, here we neglected the diffusion from the smaller faces of the sample since the increase should be mainly affected by that from the largest face because of the sample shape.

Next, we discuss the diffusion of the OH groups at the interface of the core and cladding glass. For the discussion, we need the α_{OH} values at specific positions in the glass. The α_{OH} of the polished part ($\alpha_{OH\text{-}p}$) can be estimated as follows. First, we denote the average α_{OH} of start composite as $\alpha_{OH\text{-}all}$. Next, when the α_{OH} of residual glass after the first polishing is denoted as $\alpha_{OH\text{-}r1}$, the average α_{OH} of the polished part ($\alpha_{OH\text{-}p1}$) can be written by

$$\alpha_{OH\text{-}p1} = \alpha_{OH\text{-}all} - \alpha_{OH\text{-}r1}. \tag{14}$$

Then the average α_{OH} of the lost part at the second polishing ($\alpha_{OH\text{-}p2}$) is written by using that of the residual part ($\alpha_{OH\text{-}r2}$):

$$\alpha_{OH\text{-}p2} = \alpha_{OH\text{-}all} - \alpha_{OH\text{-}r2} - \alpha_{OH\text{-}p1} = \alpha_{OH\text{-}r1} - \alpha_{OH\text{-}r2}. \tag{15}$$

For the subsequent processes, we obtained the $\alpha_{OH\text{-}p}$ in the same way as the $\alpha_{OH\text{-}p2}$ estimation. Figure 13 shows the relationship between the average α_{OH} of the polished (lost) part and polishing amount from the top surface of the core glass. Near the core glass surface, the $\alpha_{OH\text{-}p}$ increased toward the surface direction. This indicates the solution of the OH groups from the air atmosphere to the glass inside. The dashed line in the figure represents the core-cladding interface. At the part near the interface, the $\alpha_{OH\text{-}p}$ also increased toward the interface direction. Since the cladding glass is considered to be sufficiently thick for preventing the OH diffusion from the bottom surface, this indicates the diffusion of the OH groups from the water-rich cladding glass to the water-poor core. Consequently, the dehydration of the cladding glassed is also desired when the glass preform is reheated for the fiber fabrication.

V. CONCLUSION

Er-doped Bi_2O_3-based glasses were prepared and the interaction between the Er^{3+} ions and OH groups in the glasses was investigated. The total decay rate of the $^4I_{13/2}$ level of Er^{3+} ion increased with the water content, and the increase was larger for the samples doped with higher Er. It is con-

firmed that the OH groups were dominant quenching centers of excited Er^{3+} ions and a cause of concentration quenching. From the analyses of the total decay rate, the constants of relaxation via the OH groups were estimated. The constants of the Bi_2O_3-based glasses were smaller than that of other glasses.

The solution of the OH group to the Bi_2O_3-based glasses was investigated in various processes. The amounts of the OH groups were affected by the atmosphere that the glasses were melted in. The OH groups were removed in the melting process using dry gas. It is revealed that reheating processes for fiber fabrication can be also a cause of the solution of the OH groups. From the glass surface, they diffused with an order of millimeters when the glasses were annealed above softening temperature. In addition, it is suggested that the OH groups can diffuse between the core and cladding glass interface when the OH amount of each glass is different. For the better gain performance, not only the dehydration of the core glass but also that of the cladding is needed.

We fabricated highly Er doped, 5 cm length compact *C*-band fiber amplifiers with various OH concentrations. By removing the OH groups in the core glasses, the gain characteristics drastically improved and a 10 dB gain at 1560 nm was achieved with 150 mW pumping at 980 nm. The gain properties were simulated using calculated relaxation rate via the OH groups, W_{OH}, and simulation results fit the experimental ones.

[1]G. E. Keiser, Opt. Fiber Technol. **5**, 3 (1999).
[2]N. Sugimoto, Y. Kuroiwa, K. Ochiai, S. Ohara, Y. Fukasawa, S. Ito, S. Tanabe, and T. Hanada, Proceedings of Optical Amplifiers and their Applications (OAA'2000) (Optical Society of America, Quebec City, Canada, 2000), PDP3.
[3]Y. Kondo, M. Ono, J. Kageyama, M. Reyes, H. Hayashi, and N. Sugimoto, Proceedings of Optical Fiber Communication Conference (OFC'2005) (Optical Society of America, Anaheim, California, 2005), PDP2.
[4]S. Jiang *et al.*, Proceedings of Optical Amplifiers and Their Applications (OAA'2002) (Optical Society of America, Vancouver, Canada, 2002), PDP8.
[5]R. Sprengard *et al.*, Proceedings of European Conference on Optical Communications (ECOC'2002) (COM Center, Copenhagen, Denmark, 2002).
[6]P. Myslinski, D. Nguyen, and J. Chrostowski, J. Lightwave Technol. **15**, 112 (1997).
[7]P. Blixt, J. Nilsson, T. Carlnas, and B. Jaskorzynska, IEEE Photonics Technol. Lett. **3**, 996 (1991).
[8]S. Tanabe, N. Sugimoto, S. Ito, and T. Hanada, J. Lumin. **87–89**, 670 (2000).
[9]N. Sugimoto, J. Am. Ceram. Soc. **85**, 1083 (2002).
[10]X. Feng, S. Tanabe, and T. Hanada, J. Non-Cryst. Solids **281**, 48 (2001).
[11]H. Sholze, Glastech. Ber. **32**, 81 (1959).
[12]E. Snoeks, P. G. Kik, and A. Polman, Opt. Mater. (Amsterdam, Neth.) **5**, 159 (1996).
[13]V. P. Gapontsev, A. A. Izyneev, Yu. E. Sverchov, and M. R. Syrtlanov, Sov. J. Quantum Electron. **11**, 1101 (1981).
[14]H. Ebendorff-Heidepriem, W. Seeber, and D. Ehrt, J. Non-Cryst. Solids **183**, 191 (1995).
[15]S. N. Houde-Walter, P. M. Peters, J. F. Stebbins, and Q. Zeng, J. Non-Cryst. Solids **286**, 118 (2001).
[16]S. Dai, C. Yu, G. Zhou, J. Zhang, G. Wang, and L. Hu, J. Lumin. **117**, 39 (2006).
[17]Bell Communications Research, Generic requirements GR-1221-CORE, Issue 1 (1994).
[18]P. C. Becker, N. A. Olsson, and J. R. Simpson, *Erbium-Doped Fiber Amplifiers: Fundamentals and Technology* (Academic, New York 1999).
[19]H. Hayashi, N. Sugimoto, and S. Tanabe, Opt. Fiber Technol. (in press).
[20]W. L. Barnes, R. I. Laming, E. J. Tarbox, and P. R. Mokel, IEEE J. Quantum Electron. **27**, 1004 (1991).
[21]J. Nilsson, P. Blixt, B. Jaskorzynska, and J. Babonas, J. Lightwave Technol. **13**, 341 (1995).
[22]R. S. Quimby, Appl. Opt. **30**, 2546 (1991).
[23]M. Tomozawa, D. Kim, A. Agarwal, and K. M. Davis, J. Non-Cryst. Solids **288**, 73 (2001).
[24]S. Sakka, T. Kamiya, and K. Kamiya, Yogyo Kyokaishi **90**, 585 (1982).
[25]L. Nemec and J. Gotz, J. Am. Ceram. Soc. **82**, 2762 (1970).
[26]C. B. Layne, W. H. Lowdermilk, and M. J. Weber, Phys. Rev. B **16**, 10 (1977).